

# Arteriosclerosis, Thrombosis, and Vascular Biology

JOURNAL OF THE AMERICAN HEART ASSOCIATION



## **Proteomic Analysis of Defined HDL Subpopulations Reveals Particle-Specific Protein Clusters: Relevance to Antioxidative Function**

W. Sean Davidson, R.A. Gangani D. Silva, Sandrine Chantepie, William R. Lagor, M. John Chapman and Anatol Kontush

*Arterioscler. Thromb. Vasc. Biol.* 2009;29;870-876; originally published online Mar 26, 2009;

DOI: 10.1161/ATVBAHA.109.186031

Arteriosclerosis, Thrombosis, and Vascular Biology is published by the American Heart Association, 7272 Greenville Avenue, Dallas, TX 75214

Copyright © 2009 American Heart Association. All rights reserved. Print ISSN: 1079-5642. Online ISSN: 1524-4636

The online version of this article, along with updated information and services, is located on the World Wide Web at:

<http://atvb.ahajournals.org/cgi/content/full/29/6/870>

Data Supplement (unedited) at:

<http://atvb.ahajournals.org/cgi/content/full/ATVBAHA.109.186031/DC1>

Subscriptions: Information about subscribing to Arteriosclerosis, Thrombosis, and Vascular Biology is online at

<http://atvb.ahajournals.org/subscriptions/>

Permissions: Permissions & Rights Desk, Lippincott Williams & Wilkins, a division of Wolters Kluwer Health, 351 West Camden Street, Baltimore, MD 21202-2436. Phone: 410-528-4050. Fax: 410-528-8550. E-mail:

[journalpermissions@lww.com](mailto:journalpermissions@lww.com)

Reprints: Information about reprints can be found online at

<http://www.lww.com/reprints>

## Proteomic Analysis of Defined HDL Subpopulations Reveals Particle-Specific Protein Clusters Relevance to Antioxidative Function

W. Sean Davidson, R.A. Gangani D. Silva, Sandrine Chantepie, William R. Lagor,  
M. John Chapman, Anatol Kontush

**Objective**—Recent proteomic studies have identified multiple proteins that coisolate with human HDL. We hypothesized that distinct clusters of protein components may distinguish between physicochemically-defined subpopulations of HDL particles, and that such clusters may exert specific biological function(s).

**Methods and Results**—We investigated the distribution of proteins across 5 physicochemically-defined particle subpopulations of normolipidemic human HDL (HDL2b, 2a, 3a, 3b, 3c) fractionated by isopycnic density gradient ultracentrifugation. Liquid chromatography/electrospray mass spectrometry identified a total of 28 distinct HDL-associated proteins. Using an abundance pattern analysis of peptide counts across the HDL subfractions, these proteins could be grouped into 5 distinct classes. A more in-depth correlational network analysis suggested the existence of distinct protein clusters, particularly in the dense HDL3 particles. Levels of specific HDL proteins, primarily apoL-I, PON1, and PON3, correlated with the potent capacity of HDL3 to protect LDL from oxidation.

**Conclusions**—These findings suggest that HDL is composed of distinct particles containing unique (apolipo)protein complements. Such subspeciation forms a potential basis for understanding the numerous observed functions of HDL. Further work using additional separation techniques will be required to define these species in more detail. (*Arterioscler Thromb Vasc Biol.* 2009;29:870-876.)

**Key Words:** high density lipoprotein ■ mass spectrometry ■ compositional heterogeneity ■ proteome ■ oxidation

Human plasma high-density lipoprotein (HDL) particles have been classically defined as a group of pseudomicellar quasi-spherical protein/lipid complexes with hydrated densities in the range of 1.063 to 1.210 g/mL.<sup>1</sup> Overall, HDL is protein-rich compared to other plasma lipoproteins, with a protein/lipid ratio ranging from 1:2 in large light HDL2 to 10:1 in small dense pre- $\beta$ HDL.<sup>2</sup> Apolipoprotein A-I (apoA-I) is the most common protein constituent,<sup>3</sup> accounting for approximately 70% of HDL protein mass, with apoA-II comprising 15% to 20%.<sup>4</sup> The remaining 10% to 15% of protein mass is composed of minor amphipathic proteins, including apoC, apoE, apoD, apoM, and apoA-IV, with enzymes and lipid transfer proteins such as lecithin:cholesterol acyl transferase (LCAT) and cholesteryl ester transfer protein (CETP). Recent proteomic studies<sup>5–8</sup> have however identified up to 75 distinct proteins associated with centrifugally-isolated HDL. Intriguingly, the plasma abundance of most of these proteins is insufficient to permit one copy per HDL particle, suggesting that specific proteins may

be bound to distinct particle species which are differentially distributed across the HDL density spectrum.

The potential for distinct particle subpopulations is consistent with the fact that HDL exerts multiple biological activities.<sup>4</sup> Furthermore, specific molecular lipid species are distributed nonuniformly across HDL particle subpopulations; indeed, sphingosine-1-phosphate is enriched in dense HDL3.<sup>9</sup> The promotion of cholesterol efflux from peripheral tissues, including the arterial wall, with delivery to the liver for catabolism in the process of reverse cholesterol transport (RCT), is a well-established antiatherogenic function of HDL.<sup>10</sup> HDL also protects LDL from oxidative modification, decreases adhesion molecule expression in endothelial cells, and exerts antiapoptotic, antithrombotic, and antiinfectious activities.<sup>4</sup> HDL particles may also contain proteins with known roles in complement regulation, protease inhibition, and inflammation.<sup>8</sup>

Although the compositional and functional heterogeneity of HDL particles is well known, HDL is often regarded as a single entity whose plasma levels are reflected by measure-

Received December 18, 2008; revision accepted March 6, 2009.

From the Department of Pathobiology and Laboratory Medicine (W.S.D., R.A.G.D.S.), University of Cincinnati, Ohio; Université Pierre et Marie Curie-Paris 6 (S.C., M.J.C., A.K.), Paris, France; AP-HP (S.C., M.J.C., A.K.), Groupe hospitalier Pitié-Salpêtrière, Paris, France; INSERM (S.C., M.J.C., A.K.), Dyslipoproteinemia and Atherosclerosis Research Unit 551, Paris France; and the Institute for Translational Medicine and Therapeutics (W.R.L.), University of Pennsylvania, Philadelphia.

Correspondence to Dr W. Sean Davidson, Department of Pathobiology and Laboratory Medicine, University of Cincinnati, Cincinnati OH 45221. E-mail Sean.Davidson@UC.edu

© 2009 American Heart Association, Inc.

*Arterioscler Thromb Vasc Biol* is available at <http://atvb.ahajournals.org>

DOI: 10.1161/ATVBAHA.109.186031

ment of HDL-cholesterol (HDL-C). Indeed, a host of pharmacological strategies which raise HDL-C have been evaluated without regard either to the functional specificity of HDL particles or to HDL particle heterogeneity.<sup>11</sup> We hypothesized that the multiple biological functions of HDL are mediated by distinct particle subspecies defined by specific cluster(s) of bound proteins, and that such protein clusters cofractionate on isolation of HDL subpopulations. Indeed, this concept is strikingly exemplified by the capacity of a distinct subset of dense HDL3 particles that carries apoA-I, apoL-I, and haptoglobin-related protein (Hrp) to neutralize the protozoan *Trypanosoma brucei*,<sup>12</sup> the organism that causes African sleeping sickness. As an initial step toward assessing this hypothesis, plasma HDL was subfractionated into 5 physicochemically-defined particle subpopulations by isopycnic density gradient ultracentrifugation and then evaluated the respective protein moieties by mass spectrometry. This revealed that HDL-associated proteins were distributed in distinct patterns across the HDL particle subpopulations. Moreover, the potent antioxidative activity of dense HDL3 particles was characterized by a proteome of distinct composition.

## Methods

### Blood Sampling

Venous plasma from normolipidemic healthy male volunteers, with EDTA as the anticoagulant, was collected as described in online supplement at <http://atvb.ahajournals.org>. Two independent sets of samples were analyzed; the first was composed of 9 individual healthy normolipidemic donors, and the second of 3 samples, each consisting of a pool from 20 individual healthy normolipidemic donors.

### Isolation of Lipoproteins

Lipoproteins were fractionated by isopycnic density gradient ultracentrifugation as previously described.<sup>13,14</sup> Five major subfractions of HDL were isolated, ie, light HDL2b (d 1.063 to 1.087 g/mL) and HDL2a (d 1.088 to 1.110 g/mL), and dense HDL3a (d 1.110 to 1.129 g/mL), HDL3b (d 1.129 to 1.154 g/mL), and HDL3c (d 1.154 to 1.170 g/mL).<sup>9</sup> The 9 individual plasma samples were directly subjected to our density gradient fractionation protocol, whereas total HDL fraction (d 1.063 to 1.21 g/mL) was first isolated from the 3 plasma pools by sequential flotation ultracentrifugation and then fractionated by the density gradient protocol.

### Analysis of Lipoproteins

Total protein, total cholesterol (TC), free cholesterol, phospholipids, and triglyceride contents of the lipoprotein fractions were determined using commercially available enzymatic assays.<sup>15,16</sup> Apo A-I and apo A-II concentrations were determined by immunonephelometry.<sup>15,16</sup> The paraoxonase (PON) 1 activity of HDL subfractions (100 µg protein/mL) was determined photometrically in the presence of CaCl<sub>2</sub> (1 mmol/L) using phenyl acetate as a substrate.<sup>15,16</sup> Apolipoprotein F levels were monitored by Western blot analysis as described in the online supplement. The antioxidative activities of HDL subfractions were assessed as the capacity to attenuate the oxidation of reference LDL by 2,2'-azobis-(2-amidinopropane) hydrochloride (AAPH) as described elsewhere.<sup>16</sup>

### Mass Spectrometry

Delipidated, reduced, and carboxymethylated HDL protein (20 to 30 µg), determined by absorbance at 280 nm, was digested by sequencing grade trypsin at 5% of protein by wt (Promega) and incubated overnight at 37°C. 30 pmol (using an average MW for HDL proteins of 25 000) was injected onto a C18 capillary reversed phase column and analyzed with a Sciex/Applied Biosystems QSTAR XL mass

spectrometer equipped with an electrospray ionizer (ESI-MS) and a quadrupole time-of-flight (Q-ToF) dual analyzer. The MS/MS data were used to probe the SwissProt human database using 3 different search engines followed by manual evaluation of ambiguous peptide assignments. This identification strategy was verified using the Universal Proteomics Standard (Sigma). Spectral counting of the total peptides identified was used to compare relative protein abundances of the same protein between samples. See the online supplement for details of the MS and the analysis strategy.

### Statistical Analysis

All data are shown as means ± 1 sample SD. Pearson moment-product correlation coefficients were calculated to evaluate relationships between variables. Correlations among HDL proteins across the density subfractions were additionally analyzed using the organic algorithm of the Cytoscape software package. The nodes were laid out and modified to cluster highly correlated nodes in close proximity.

## Results

### Identification of Protein Components of Human HDL Particle Subpopulations

To determine the distribution of specific proteins among 5 particle subpopulations of human HDL, 3 pooled plasma samples (derived from 20 donors each) and 9 nonpooled individual plasma samples were ultracentrifugally fractionated on a density gradient. These HDL particle subfractions have been extensively characterized in terms of their chemical composition, physical properties, and biological functions.<sup>9,15-17</sup> A representative gel electrophoretic analysis of the native HDL subfractions isolated from pooled plasma is shown in supplemental Figure I. The average diameters of the HDL particles ranged from about 8.0 nm for the densest HDL3c fractions to about 12 nm for the lightest HDL2b fractions. Compositional data for these subfractions are shown in supplemental Table I and confirm data published elsewhere.<sup>9,15,16</sup>

The isolated HDL particle subpopulations were subjected to ESI-MS. Figure 1 shows the total protein components identified across all 5 subfractions in both the individual and pooled samples (see Methods). The total peptide counts for each protein are listed in supplemental Tables II and III. In the pooled samples, which were first subjected to fractionation by sequential ultracentrifugation and then by the isopycnic density gradient procedure, we identified 22 distinct proteins on the basis of our analytic criteria. Twenty-eight protein species were identified in plasma samples from individual donors, which had been fractionated by single density gradient ultracentrifugation; these included the majority of the apolipoproteins previously established to associate with ultracentrifugally-isolated HDL.<sup>5-8</sup> Peptides derived from apoA-I predominated, as expected. We also identified apoB and apo(a) in the least dense HDL fractions which likely represents lipoprotein(a) contamination (see below). It is noteworthy that we did not observe several complement factors and protease inhibitors that were documented in earlier proteomic studies.<sup>5-8</sup> Finally, platelet basic protein was identified as a potentially new HDL-associated protein.

There is substantial evidence that the process of ultracentrifugation can alter the composition of HDL by disrupting protein-protein or protein-lipid associations through exposure to high ionic strength and extreme g-forces for prolonged

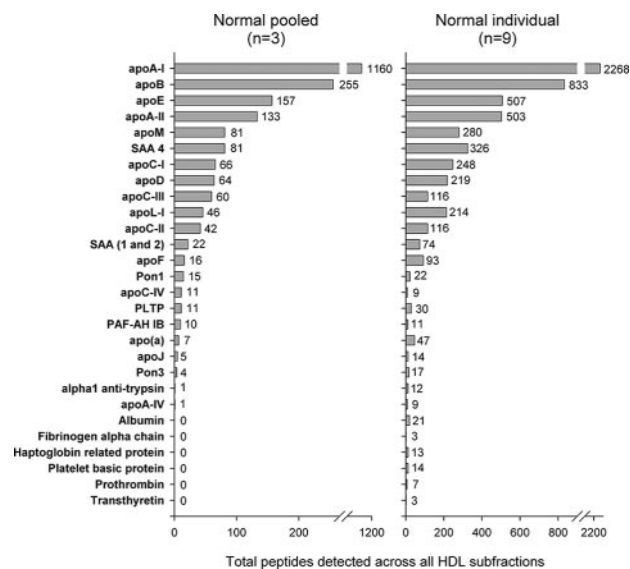


**Figure 1.** Total peptides found for each protein, irrespective of HDL subclass. Left, Summed from 3 samples derived from the pooled plasma from 20 normolipidemic donors. Right, Summed from 9 individual normolipidemic plasma samples. apo indicates apolipoprotein; SAA, serum amyloid alpha; Pon, paraoxonase; PLTP, phospholipid transfer protein; PAF-AH, platelet activating factor-aryl hydrolase subunit 1B.

periods.<sup>18</sup> The presence of several proteins in the single isopycnic density gradient separation that were not detected after the consecutive sequential and density gradient separations (Figure 1) suggests that the former procedure may result in less perturbation of native lipoprotein structure.

### Protein Distribution Across HDL Density Subpopulations

We next asked whether the total peptide counts could serve as an index of the relative abundance of a given protein species across HDL subfractions. In the absence of stable isotopes or other standardization methods, MS is not an inherently quantitative technique. However, because the same amount of total protein in each HDL subfraction was injected into the mass spectrometer, we reasoned that the total peptide counts for a given protein should be proportional to the amount of that protein present in the sample. Indeed, this approach has been used successfully before.<sup>19,20</sup> To test this, we performed parallel quantitative analyses for several of the identified proteins and compared the relative abundance to that determined by total MS peptide counts (note that both the MS and biochemical analyses were performed on the same physical sample). Figure 2A shows data obtained for apoA-II as an example; peptide counts determined by MS provided a similar abundance pattern to that obtained by nephelometric analysis across HDL subfractions. The peptide patterns determined by both methods were highly correlated (Figure 2A, right panels). We also compared MS peptide counts with activity measurements for PON1 (Figure 2B) and again were able to demonstrate a strong correlation. Finally, the MS peptide count for apoF was compared with a Western blot of the same subfractions. ApoF was specific to the HDL3c subfraction in this donor by both MS and Western blot analyses. These data indicate that MS peptide counts

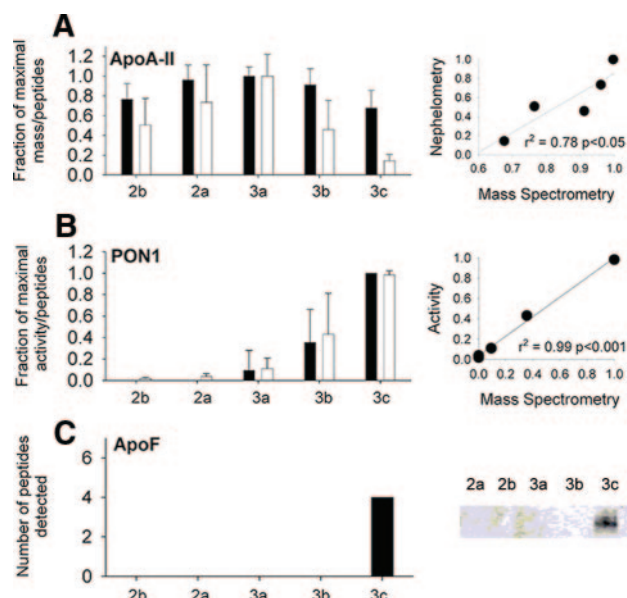


**Figure 2.** MS peptide counts as an index of relative protein abundance. A, Averaged MS peptide counts (white) vs apoA-II mass determined by immunonephelometry (black). The subfraction with max. peptide count was set to 1.0, and the others were scaled accordingly. The plot (right) correlates normalized nephelometry data (y axis) with MS data (x axis) ( $n=7$ ). B, MS peptide counts vs paroxonase activity measurement ( $n=6$ ). C, MS peptide counts vs a Western blot for apoF ( $n=1$ ). Error bars=1 SD.

provide a valid approach for determination of the relative abundance of a given protein across the HDL subfractions. Clearly, however, such comparisons are only valid when the same protein is compared among different HDL subfractions and we recognize that the quality of this relationship may vary for different proteins, especially small ones with difficult-to-detect peptides.

Using the MS peptide counts to monitor the relative abundance of each protein, HDL-associated proteins were arbitrarily grouped into 5 distinct patterns of relative abundance across HDL subpopulations (Figure 3). The most frequent pattern observed involved proteins that were localized almost exclusively in the densest HDL3b and 3c subfractions (Class A). Class B proteins were preferentially localized to the densest HDL subpopulations but were detectable in all. Class C proteins, including apoA-I and apoA-II, were distributed across all subfractions in a relatively uniform profile. Class D proteins were preferentially associated with HDL2 subpopulations of lowest density, but were nonetheless detectable in all subpopulations. Finally, apoB and apolipoprotein (a) were limited to the light HDL2 subfractions and were indications of the presence of lipoprotein (a) whose hydrated density overlaps that of HDL2.<sup>21</sup>

The analysis shown in Figure 3 compares sums of peptides accumulated from all samples for each subfraction. To begin to identify proteins that may colocalize preferentially to a given subpopulation of HDL particles, we performed a more detailed correlation analysis in which the subfraction distribution pattern for a given protein was compared to all other proteins within each of the 9 patient samples. Examples of the strongest correlations are shown in Figure 4. Based on the

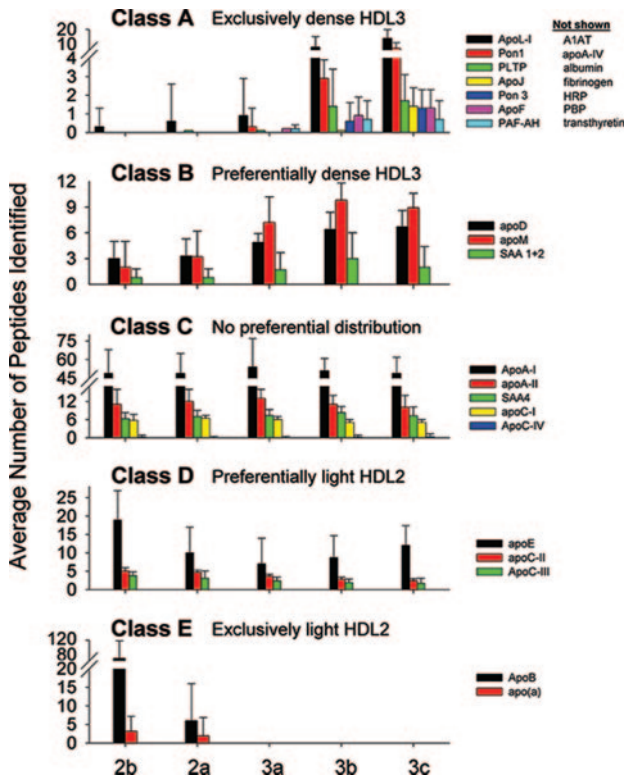


**Figure 3.** Abundance patterns of representative proteins across the HDL subpopulations. Class A, Limited to dense HDL3; those listed showed the same pattern (not shown). Class B, Prefer dense HDL3 but are in all subfractions. Class C, Evenly distributed. Class D, Prefer light HDL2 but are in all subfractions. Class E, Limited to light HDL2. Error bars=1 SD (n=9).

calculated Pearson correlation coefficient ( $r$ ), the strongest correlation occurred between PON1 and PON3. Strong correlations were similarly detected between PON1 and apoL-I, apoD, and apoM, and also between apoL-I and apoF. Figure 5 shows an organic network generated by the Cytoscape software package that graphically depicts statistically significant correlations between identified proteins (nodes) as connecting lines (edges). Weak correlations are indicated by long/thin lines, whereas strong correlations are indicated by short/thick lines; tightly correlated proteins appear in juxtaposition in the network.

### Correlations of Protein Composition With Antioxidative Activity of HDL

We have previously characterized the capacity of these HDL subpopulations to protect LDL from oxidation. Dense HDL3 fractions are most potently protective on a per particle basis among all HDL subpopulations<sup>2,15</sup> (supplemental Table 1). In the presence of HDL, LDL oxidation proceeds in a 2-step process that exhibits a “lag” phase with a slow rate of conjugated diene accumulation attributable to the presence of antioxidants, including those in HDL. A second rapid phase follows whose duration and rate is largely dependent on the antioxidative functionality of HDL. C<sub>max</sub> represents the total amount of conjugated dienes formed during the assay. We correlated the relative abundance of each protein, determined by MS peptide count, with parameters of LDL oxidation in the presence of

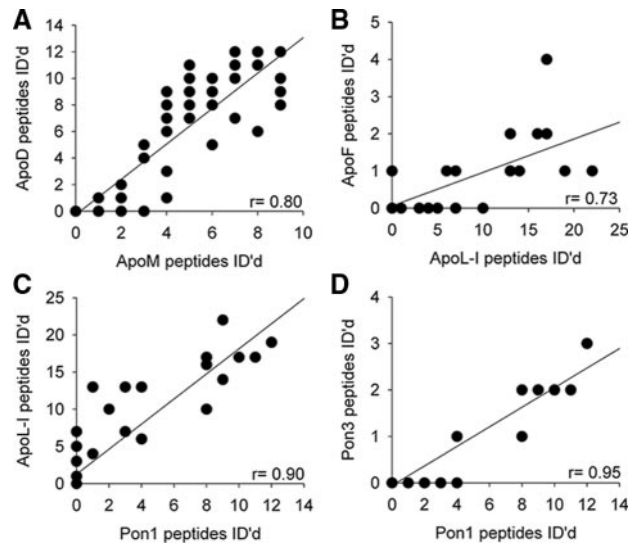


**Figure 4.** HDL protein correlations across the subfractions. The peptide counts for a given protein within each HDL subclass and subject were plotted against all other proteins to derive a Pearson correlation coefficient. Examples of 4 highly correlated pairs are shown: A, apoD vs apoM,  $P < 0.001$ . B, apoF vs apoL-I,  $P < 0.001$ . C, apoL-I vs Pon1/2,  $P < 0.001$ . D, Pon1/2 vs Pon3,  $P < 0.001$  by a 2-tailed correlation test.

individual HDL particle subfractions. Figure 6 shows the Pearson correlation coefficients for the 8 HDL proteins that exhibited a significant relationship with at least 1 of the above indices of antioxidant function. Any protein that contributes significantly to the antioxidative functionality of HDL should show positive correlations with the duration of phases 1 and 2 on the one hand, and negative correlations with the oxidation rates of phases 1 and 2 as well as with C<sub>max</sub> on the other. ApoL-I, PON1, and PON3 showed significant correlations with all 5 parameters with strong positive and negative correlations. PLTP and apoM showed a significant negative correlation only with C<sub>max</sub>. ApoJ, although not reaching significance in terms of C<sub>max</sub>, showed a positive correlation with the duration of the lag phase. SAA4 and apoD showed significant correlations with 3 of the 5 parameters.

### Discussion

Our present data reveal that: (1) HDL-associated proteins are localized in distinct patterns across physicochemically-defined particle subpopulations, as evidenced by both abundance pattern analysis of peptide counts determined by ESI-MS (Figure 3) and correlational network analysis (Figure 4 and 5), and (2) the presence of specific HDL proteins correlates with the capacity of HDL subpopulations to attenuate LDL oxidation. Our findings argue strongly for HDL particle subspeciation in terms of the HDL proteome.

The most frequent pattern distribution that we observed occurred almost exclusively in dense HDL3 (Class A). This included apoL-I, apoF, PON1/2, PLTP, apoJ, PON3, A1AT, apoA-IV, albumin, fibrinogen, Hrp, PBP, and transthyretin, the latter 4 representing minor constituents. Importantly, we observed only minimal contamination of dense HDL3 with albumin, thereby confirming our previously reported immunologic data.<sup>15</sup> Several class A proteins, namely apoL-I,<sup>22</sup> apoF (also termed lipid transfer inhibitor protein),<sup>23</sup> apoJ,<sup>24,25</sup>

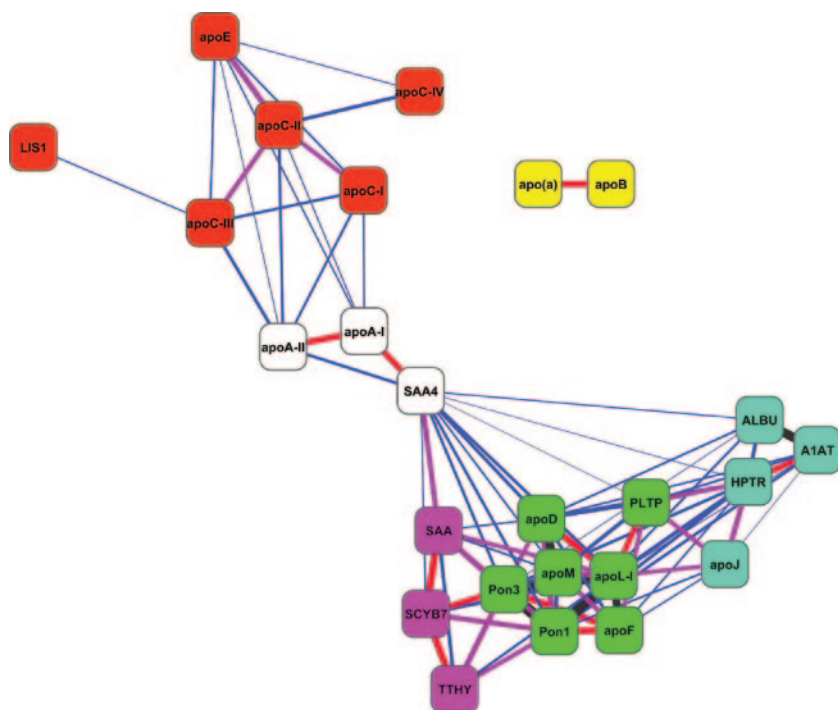


**Figure 5.** HDL proteins correlational network. Each statistically significant correlation between HDL-associated proteins (nodes) is represented as a line (edge) with a thickness proportional to the Pearson coefficient ( $r$ ) of the correlation (blue  $0.3 < r < 0.5$ , purple  $0.5 < r < 0.6$ , red  $0.6 < r < 0.7$ , and black  $r > 0.7$ ). The nodes were treated like physical objects with mutually repulsive forces connected by metal springs representing the experimentally derived correlations; the sum of the forces emitted by the nodes and edges reaches a local minimum. The nodes were colored according to putative clusters determined visually. Lis1 refers to PAF-AH subunit 1B; A1AT,  $\alpha$ -1-antitrypsin; HPTR, haptoglobin related protein; TTHY, transthyretin; SCYB7 (CXCL7), platelet binding protein precursor.

PON1,<sup>15,25</sup> and apoA-IV,<sup>26,27</sup> have previously been reported to associate with centrifugally-isolated HDL3. Indeed, apoL-I, a major component of the trypanosome lytic factor of human serum, coisolates with dense HDL particles (d 1.21 to 1.24 g/mL) which also contain apoA-I, apoA-II, apoC-I, apoC-II, apoC-III, and Hrp.<sup>12,22</sup> The efficient function of such particles in the lysis of trypanosomes requires the presence of both Hrp and apoA-I.<sup>12</sup> In a similar fashion, apoF coisolates with dense HDL (mean density, 1.134 g/mL) which also contain apoA-I, apoC-II, apoE, apoJ, apoD, and PON1.<sup>23</sup> PON1, a hydrolytic antiatherogenic enzyme with major lactonase activity, is mainly confined to dense HDL (d >1.15 g/mL) containing apoA-I and apoJ.<sup>15,25,28</sup> It is reasonable to expect that PON3, being closely related to PON1, is similarly distributed across HDL subpopulations. Finally, apoA-IV, an apolipoprotein with antiatherogenic, antioxidative, and lipolytic properties, is also present mainly on dense HDL particles.<sup>26,27</sup>

Class B proteins preferentially associated with dense HDL3 but were also detectable at lower levels in HDL2.

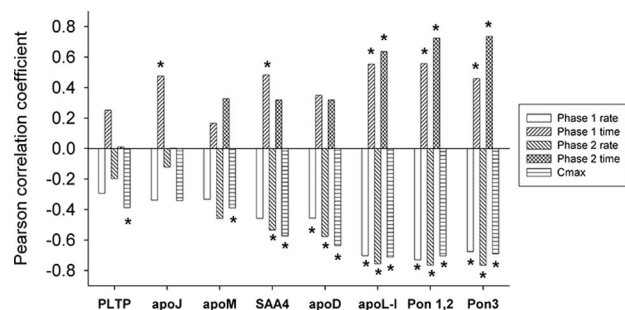


**Figure 6.** HDL proteins related to LDL oxidation protection. Peptide counts were correlated against 5 parameters (see text) that describe the kinetics of LDL oxidation by AAPH in the presence of each HDL subfraction. Proteins demonstrating significant Pearson correlation coefficients with at least 1 parameter are shown; \* $P < 0.05$ .

ApoM,<sup>29</sup> apoD,<sup>21</sup> and SAA 1/2<sup>30,31</sup> are known to coisolate with dense HDL3. Indeed, apoM, a member of the lipocalin protein superfamily which may bind small lipophilic ligands, is a significant component of small dense prebeta HDL particles involved in cellular cholesterol efflux.<sup>29</sup> ApoD is another member of the lipocalin family displaying the properties of a multi-ligand multi-functional transporter.<sup>32</sup> Such functional resemblance of apoM and apoD, considered together with strong correlations between their abundance, may suggest physical association on a subclass of dense protein-rich small HDL particles, one of whose principal functions involves transport of small hydrophobic molecules.

Two classes of proteins were preferentially localized to light HDL2. First, apoB and apo(a) were exclusively detected in large light HDL2b and 2a (Class E), indicative of the overlap in hydrated densities between HDL2 and Lp(a).<sup>21</sup> Second, apoE, apoC-I, apoC-II, and apoC-III preferentially localized to light HDL2, but were present in all HDL subfractions (Class D). The preference of apoE and apoCs for large light HDL2 is well established.<sup>33,34</sup> ApoE is a key HDL apolipoprotein involved in the interaction of HDL with cellular receptors of the LDL receptor family.<sup>35</sup> ApoE-rich, large, light HDL are implicated in the RCT pathway as ligands for scavenger receptor type B class I (SR-BI) and ATP-binding cassette transporter G1 (ABCG1).<sup>36</sup> The presence of apoCs in such particles may endow them with additional capacities to modulate RCT—eg, through the inhibition of CETP by apoC-I, activation of LPL by apoC-II, or inhibition of LPL by apoC-III.

Finally, a number of proteins were uniformly distributed across the subpopulations (Class C); these included apoA-I and apoA-II, consistent with their postulated roles in the structural organization and metabolism of HDL particles.<sup>3,37</sup> The absence of apparent segregation of SAA4 and apoC-IV

between HDL particle subpopulations represents a less obvious finding and may reflect the absence of specific interactions between any of these proteins and other HDL components.

When we performed the correlational network analysis that looked for cooccurrences of any 2 proteins within each subject, we observed strong relationships between proteins within each abundance pattern class described above. For example, the class A proteins apoL-I, PON1, PON3, and apoF demonstrated strong intercorrelations (Figure 5). Interestingly, this analysis also revealed strong correlations between these proteins and apoM and apoD, both class B proteins. Such tight relationships may be suggestive of distinct protein clusters defining separate HDL particle entities. Potential clusters suggested by the current network analysis are shown in different colors in Figure 5. Note that apoB and apo(a) clustered to a separate net with no relationships with any of the other proteins. As stated above, we believe that this represents lipoprotein(a) contamination in our HDL2 samples. Because apoB and apo(a) are covalently associated, the fact that these 2 proteins segregated to a separate network serves as an internal control and suggests that the correlation strategy is indeed capable of distinguishing distinct particles within the fractions. It should be cautioned, however, that the analysis of only 5 subfractions leaves a distinct possibility that some of the relationships apparent in Figure 5 may have resulted from coincidental cofractionation of proteins that are not necessarily present on the same HDL particle. Furthermore, a limitation of the present experimental approach involves the potential for ultracentrifugation to induce redistribution of weakly-bound proteins by gravitational forces or high ionic strength. Further studies using separation strategies that target alternative physicochemical properties of the particles and more extensive fractionation will be required to more rigorously identify cosegregating proteins. Despite these limitations, however, the current studies are supportive of the idea that HDL is an ensemble of distinct particles distinguished by discrete protein complements.

The potential functional relevance of the clustering of HDL proteins is further underlined by the significant correlations observed between the abundances of several proteins enriched in dense HDL3 and the capacity of HDL to attenuate LDL oxidation. The strong correlations observed with PON3, PON1/2, and apoL-I suggest that dense HDL3 particles carrying these proteins display particularly potent antioxidative activity, consistent with earlier findings.<sup>15,16</sup> The role of paraoxonases in the direct protection of LDL from oxidative stress is controversial at present (see Kontush and Chapman<sup>4</sup> for discussion); by contrast, no data exist on the potential antioxidative properties of apoL-I. It remains therefore to be determined whether these proteins, or apoD, SAA4, apoM, apoJ, and PLTP, directly participate in the inhibition of LDL oxidation or rather whether they represent markers of dense HDL3 particles with elevated antioxidative activity. It should be also kept in mind that the free-radical generating system (AAPH) used in our studies represents a chemical model of free-radical fluxes in the arterial intima, whose physiological relevance is not firmly established despite widespread use.<sup>15,38</sup> It

remains therefore theoretically possible that additional HDL proteins could also contribute to the HDL-mediated protection of LDL from oxidation in the arterial wall.

In conclusion, we propose that the protein clusters detected herein may be indicative of distinct subsets of HDL particles which display specific biological function(s). At this point, it is not clear what drives the segregation of HDL proteins among the subparticles, but 2 likely possibilities include: (1) specific protein:protein interactions on the particle surface, or (2) the attraction of certain proteins to a particular particle biophysical characteristic, such as lipid packing density or surface curvature. Our data are thus inconsistent with the view that HDL is simply a random association of pseudomicellar lipid particles with rapidly exchanging apolipoproteins. In agreement with Shiflett et al,<sup>12</sup> we support the concept that HDL may serve as a platform for the assembly of certain protein components which perform specific function(s); and, as originally hypothesized by Marcel et al,<sup>39</sup> our data suggest that apolipoproteins form the basis for functional heterogeneity of HDL.

There is a potential for both the proteome and lipidome of HDL particles to differ between healthy populations and those at elevated cardiovascular risk. Elucidation of the mechanistic basis of functional HDL deficiency may provide novel strategies to improve HDL functionality with proteomic studies relating HDL composition to function representing an invaluable approach. Our work raises the exciting possibility that monitoring the presence or absence of combinations of interacting proteins may provide better biomarkers of HDL function than simply measuring plasma levels of any one component alone.

### Sources of Funding

This work was supported by U.S. National Institutes of Health (WSD HL67093), the French National Institute for Health and Medical Research (INSERM), Agence Nationale de la Recherche (COD 2005 Lisa), and Association Pour la Recherche sur les Lipoprotéines et l'Athérosclérose, A.K. and W.S.D. were supported by International High Density Lipoprotein Research Awards from Pfizer (USA). M.J.C. and A.K. gratefully acknowledge the award of a Contrat d'Interface from Assistance Publique - Hôpitaux de Paris/INSERM (France).

### Disclosures

None.

### References

1. Havel RJ, Eder HA, Bragdon JH. The distribution and chemical composition of ultracentrifugally separated lipoproteins in human serum. *J Clin Invest.* 1955;34:1345–1353.
2. Kontush A, Chapman MJ. Antiatherogenic small, dense HDL - guardian angel of the arterial wall? *Nat Clin Pract Cardiovasc Med.* 2006;3:144–153.
3. Davidson WS, Thompson TB. The structure of apolipoprotein A-I in high density lipoproteins. *J Biol Chem.* 2007;282:22249–22253.
4. Kontush A, Chapman MJ. Functionally defective HDL: A new therapeutic target at the crossroads of dyslipidemia, inflammation and atherosclerosis. *Pharmacol Rev.* 2006;3:342–374.
5. Karlsson H, Leanderson P, Tagesson C, Lindahl M. Lipoproteomics II: mapping of proteins in high-density lipoprotein using two-dimensional gel electrophoresis and mass spectrometry. *Proteomics.* 2005;5:1431–1445.

6. Heller M, Stalder D, Schlappritzi E, Hayn G, Matter U, Haeberli A. Mass spectrometry-based analytical tools for the molecular protein characterization of human plasma lipoproteins. *Proteomics*. 2005;5:2619–2630.
7. Rezaee F, Casetta B, Levels JH, Speijer D, Meijers JC. Proteomic analysis of high-density lipoprotein. *Proteomics*. 2006;6:721–730.
8. Vaisar T, Pennathur S, Green PS, Gharib SA, Hoofnagle AN, Cheung MC, Byun J, Vuletic S, Kassim S, Singh P, Chea H, Knopp RH, Brunzell J, Geary R, Chait A, Zhao XQ, Elkon K, Marcovina S, Ridker P, Oram JF, Heinecke JW. Shotgun proteomics implicates protease inhibition and complement activation in the antiinflammatory properties of HDL. *J Clin Invest*. 2007;117:746–756.
9. Kontush A, Therond P, Zerrad A, Couturier M, Negre-Salvayre A, de Souza JA, Chantepie S, Chapman MJ. Preferential sphingosine-1-phosphate enrichment and sphingomyelin depletion are key features of small dense HDL3 particles: relevance to antiapoptotic and antioxidative activities. *Arterioscler Thromb Vasc Biol*. 2007;27:1843–1849.
10. Lewis GF, Rader DJ. New insights into the regulation of HDL metabolism and reverse cholesterol transport. *Circ Res*. 2005;96:1221–1232.
11. Kontush A, Guerin M, Chapman MJ. Spotlight on HDL-raising therapies: insights from the torcetrapib trials. *Nat Clin Pract Cardiovasc Med*. 2008;5:329–336.
12. Shiflett AM, Bishop JR, Pahwa A, Hajduk SL. Human high density lipoproteins are platforms for the assembly of multi-component innate immune complexes. *J Biol Chem*. 2005;280:32578–32585. Epub 32005 Jul 32526.
13. Chapman MJ, Goldstein S, Lagrange D, Laplaud PM. A density gradient ultracentrifugal procedure for the isolation of the major lipoprotein classes from human serum. *J Lipid Res*. 1981;22:339–358.
14. Guerin M, Le Goff W, Lassel TS, Van Tol A, Steiner G, Chapman MJ. Atherogenic role of elevated CE transfer from HDL to VLDL(1) and dense LDL in type 2 diabetes: impact of the degree of triglyceridemia. *Arterioscler Thromb Vasc Biol*. 2001;21:282–288.
15. Kontush A, Chantepie S, Chapman MJ. Small, dense HDL particles exert potent protection of atherogenic LDL against oxidative stress. *Arterioscler Thromb Vasc Biol*. 2003;23:1881–1888.
16. Hansel B, Giral P, Nobecourt E, Chantepie S, Bruckert E, Chapman MJ, Kontush A. Metabolic syndrome is associated with elevated oxidative stress and dysfunctional dense high-density lipoprotein particles displaying impaired antioxidative activity. *J Clin Endocrinol Metab*. 2004;89:4963–4971.
17. Goulinet S, Chapman MJ. Plasma LDL and HDL subspecies are heterogeneous in particle content of tocopherols and oxygenated and hydrocarbon carotenoids. Relevance to oxidative resistance and atherogenesis. *Arterioscler Thromb Vasc Biol*. 1997;17:786–796.
18. Kunitake ST, Kane JP. Factors affecting the integrity of high density lipoproteins in the ultracentrifuge. *J Lipid Res*. 1982;23:936–940.
19. Wiener MC, Sachs JR, Deyanova EG, Yates NA. Differential mass spectrometry: a label-free LC-MS method for finding significant differences in complex peptide and protein mixtures. *Anal Chem*. 2004;76:6085–6096.
20. Old WM, Meyer-Arendt K, Aveline-Wolf L, Pierce KG, Mendoza A, Sevinsky JR, Resing KA, Ahn NG. Comparison of label-free methods for quantifying human proteins by shotgun proteomics. *Mol Cell Proteomics*. 2005;4:1487–1502.
21. Campos E, McConathy WJ. Distribution of lipids and apolipoproteins in human plasma by vertical spin ultracentrifugation. *Arch Biochem Biophys*. 1986;249:455–463.
22. Hajduk SL, Moore DR, Vasudevacharya J, Siqueira H, Torri AF, Tytler EM, Esko JD. Lysis of *Trypanosoma brucei* by a toxic subspecies of human high density lipoprotein. *J Biol Chem*. 1989;264:5210–5217.
23. He Y, Greene DJ, Kinter M, Morton RE. Control of cholesterol ester transfer protein activity by sequestration of lipid transfer inhibitor protein in an inactive complex. *J Lipid Res*. 2008;49:1529–1537.
24. de Silva HV, Stuart WD, Duvic CR, Wetterau JR, Ray MJ, Ferguson DG, Albers HW, Smith WR, Harmony JA. A 70-kDa apolipoprotein designated ApoJ is a marker for subclasses of human plasma high density lipoproteins. *J Biol Chem*. 1990;265:13240–13247.
25. Bergmeier C, Siekmeier R, Gross W. Distribution spectrum of paraoxonase activity in HDL fractions. *Clin Chem*. 2004;50:2309–2315.
26. Ohta T, Fidge NH, Nestel PJ. Studies on the in vivo and in vitro distribution of apolipoprotein A-IV in human plasma and lymph. *J Clin Invest*. 1985;76:1252–1260.
27. Bisgaier CL, Sachdev OP, Megna L, Glickman RM. Distribution of apolipoprotein A-IV in human plasma. *J Lipid Res*. 1985;26:11–25.
28. Kelso GJ, Stuart WD, Richter RJ, Furlong CE, Jordan-Starck TC, Harmony JA. Apolipoprotein J is associated with paraoxonase in human plasma. *Biochemistry*. 1994;33:832–839.
29. Wolfrum C, Poy MN, Stoffel M. Apolipoprotein M is required for prebeta-HDL formation and cholesterol efflux to HDL and protects against atherosclerosis. *Nat Med*. 2005;11:418–422.
30. Benditt EP, Eriksen N. Amyloid protein SAA is associated with high density lipoprotein from human serum. *Proc Natl Acad Sci U S A*. 1977;74:4025–4028.
31. Coetzee GA, Strachan AF, van der Westhuyzen DR, Hoppe HC, Jeenah MS, de Beer FC. Serum amyloid A-containing human high density lipoprotein 3. Density, size, and apolipoprotein composition. *J Biol Chem*. 1986;261:9644–9651.
32. Rassart E, Bedirian A, Do Carmo S, Guinard O, Sirois J, Terrisse L, Milne R. Apolipoprotein D. *Biochim Biophys Acta*. 2000;1482:185–198.
33. Schaefer EJ, Foster DM, Jenkins LL, Lindgren FT, Berman M, Levy RI, Brewer HB Jr. The composition and metabolism of high density lipoprotein subfractions. *Lipids*. 1979;14:511–522.
34. Cheung MC, Albers JJ. Distribution of high density lipoprotein particles with different apoprotein composition: particles with A-I and A-II and particles with A-I but no A-II. *J Lipid Res*. 1982;23:747–753.
35. Yancey PG, Yu H, Linton MF, Fazio S. A Pathway-Dependent on ApoE, ApoAI, and ABCA1 Determines Formation of Buoyant High-Density Lipoprotein by Macrophage Foam Cells. *Arterioscler Thromb Vasc Biol*. 2007;27:1123–1131.
36. Mahley RW, Huang Y, Weisgraber KH. Putting cholesterol in its place: apoE and reverse cholesterol transport. *J Clin Invest*. 2006;116:1226–1229.
37. Silva RA, Schneeweis LA, Krishnan SC, Zhang X, Axelsen PH, Davidson WS. The structure of apolipoprotein A-II in discoidal high density lipoproteins. *J Biol Chem*. 2007;282:9713–9721.
38. Stocker R, Keane JF Jr. Role of oxidative modifications in atherosclerosis. *Physiol Rev*. 2004;84:1381–1478.
39. Marcel YL, Weech PK, Nguyen TD, Milne RW, McConathy WJ. Apolipoproteins as the basis for heterogeneity in high-density lipoprotein2 and high-density lipoprotein3. Studies by isoelectric focusing on agarose films. *Eur J Biochem*. 1984;143:467–476.

## **Proteomic analysis of defined HDL subpopulations reveals particle-specific protein clusters: Relevance to antioxidative function**

W. Sean Davidson<sup>\*†</sup>, R.A. Gangani D. Silva<sup>\*</sup>, Sandrine Chantepie<sup>‡,§,||</sup>, William R. Lagor<sup>¶</sup>, M. John Chapman<sup>‡,§,||</sup> and Anatol Kontush<sup>‡,§,||</sup>

<sup>\*</sup> Department of Pathobiology and Laboratory Medicine, University of Cincinnati, Cincinnati OH, USA; <sup>‡</sup> Université Pierre et Marie Curie-Paris 6, Paris, F-75013 France; <sup>§</sup> AP-HP, Groupe hospitalier Pitié-Salpêtrière, Paris, F-75013 France; <sup>||</sup> INSERM, Dyslipoproteinemia and Atherosclerosis Research Unit 551, Paris F-75013 France. <sup>¶</sup> Institute for Translational Medicine and Therapeutics, University of Pennsylvania, Philadelphia, PA, USA

### **Supplement Material**

*Blood sampling.* Venous blood from normolipidemic healthy male volunteers was collected into sterile evacuated tubes (Vacutainer) in the presence or absence (to obtain serum) of EDTA (final concentration, 1.8 mg/ml) after an overnight fast. EDTA plasma was used to isolate HDL subfractions for proteomics studies in order to protect HDL from autoxidation by trace amounts of transition metals during experimental procedures.<sup>1</sup> Serum was employed to obtain HDL subfractions with intact paraoxonase (PON) activity for studies of antioxidative activity of HDL as PON is strongly inhibited by EDTA<sup>2</sup> (see below). All subjects gave informed consent; the study was performed in accordance with the Institutional Review Committee. Donors receiving antioxidant vitamin supplementation or drugs known to affect lipoprotein

metabolism were excluded as were smokers and excessive alcohol consumers. After blood collection, EDTA plasma and serum was immediately separated by centrifugation at 4°C. Two independent sets of plasma samples were analyzed in this study. The first sample set was composed of plasmas from 9 individual healthy normolipidemic donors. The second set was comprised of 3 samples, each containing plasma pooled from 20 individual healthy normolipidemic donors.

*Isolation of lipoproteins.* Plasma lipoproteins were fractionated from serum (in order to preserve the activity of paraoxonase 1 (PON1)) or EDTA plasma by isopycnic density gradient ultracentrifugation as previously described.<sup>3-5</sup> Five major subfractions of HDL were isolated, i.e. light HDL2b (d 1.063–1.087 g/mL) and HDL2a (d 1.088–1.110 g/mL), and dense HDL3a (d 1.110–1.129 g/mL), HDL3b (d 1.129–1.154 g/mL), and HDL3c (d 1.154–1.170 g/mL).<sup>6</sup> The validity and reproducibility of our density fractionation of HDL particle subspecies have been extensively documented.<sup>3-5</sup> The 9 individual plasma samples were directly subjected to a gradient fractionation protocol, whereas the 3 plasma pools were first subjected to sequential ultracentrifugation to isolate the total HDL fraction (d 1.063 – 1.21 g/ml) which was then subjected to our density gradient fractionation protocol in order to isolate HDL subfractions. Before use, KBr (and, in the case of plasma, EDTA) was removed from HDL solutions by exhaustive dialysis for 24 h at 4°C. Lipoproteins were stored at 4°C and used within 10 days.

*Lipoprotein chemical composition.* Total protein, total cholesterol (TC), free cholesterol, phospholipid and triglyceride contents of isolated lipoprotein subfractions were determined using commercially available enzymatic assays.<sup>1,7</sup> Cholesteryl ester (CE) content was calculated by multiplying the difference between total and free cholesterol by 1.67 in order to take into consideration contribution from fatty acid

moiety of CE.<sup>3-5</sup> Total protein was measured using bicinchoninic acid (Pierce/Thermo Fisher Scientific, Brebières, France). Apo A-I and apo A-II were measured using immunonephelometry.<sup>1,7</sup> PON1 activity of HDL subfractions (100 µg protein/ml) was determined photometrically in the presence of CaCl<sub>2</sub> (1 mM) using phenyl acetate as a substrate.<sup>1,7</sup>

*HDL-mediated protection of LDL against oxidation.* LDL (10 mg TC/dL) was oxidized at 37 °C in Dulbecco's PBS (pH 7.4) in the presence of 1 mM 2,2'-azobis-(2-amidinopropane) hydrochloride (AAPH); HDL subfractions (final concentration, 10 mg total mass/dl) obtained from serum were added to LDL directly before oxidation. Accumulation of conjugated dienes was measured as the increment in absorbance at 234 nm.<sup>7</sup> The kinetics of diene accumulation revealed two characteristic phases, the lag and propagation phases. For each curve, the duration of each phase, average oxidation rates within each phase and the amount of dienes formed at the end of the propagation phase (maximal amount of dienes) were calculated.

*Sample preparation for LC-MS analysis.* 150 µg of total protein from each HDL subfraction were lyophilized to dryness in borosilicate tubes. The lipids were extracted by adding 1 ml of an ice-cold 2:1 (vol:vol) mixture of chloroform:methanol followed by ultrasonic dispersal of the protein pellet and a 30 min incubation on ice. Then 1 ml of ice-cold methanol was added followed by centrifugation at 4000 x g for 30 min at 4 °C. The pellet was washed with 2 ml cold methanol and respun. The moist pellet was resuspended in 90 µl of 20% methanol/80% ammonium bicarbonate at pH 7.6. The proteins were reduced by incubation for 30 min at 42 °C in 10 mM DTT and carboxymethylated with additional 30 min incubation at room temperature with 40 mM iodoacetamide in the dark. 20 to 30 µg of the protein were then digested by sequencing grade trypsin at 5% of protein by wt (Promega) and incubated

overnight at 37 °C. The peptides were lyophilized to dryness and stored at -80 °C until analyzed by mass spectrometry. Peptides were resolubilized in 20 µl 0.1% TFA in ddwater and gently vortexed. Any particulates were pelleted in an Eppendorf microfuge set at maximum speed for 10 min. The top 15 µl was placed into an autosampler vial.

LC-MS analysis. 30 pmol (using an average MW for HDL proteins of 25,000) was injected onto a C18 capillary reversed phase column (Vydac, 500 µm X 15 cm) on a capillary HPLC (Agilent 1100) and eluted on an acetonitrile gradient of 0-40% with 0.1%TFA for 120 min at 6.0 µl/min. The eluting peaks were subjected to ESI-MS detection on a Sciex/Applied Biosystems QSTAR XL mass spectrometer equipped with an electrospray ionizer and a quadropole time-of-flight (Q-ToF) dual analyzer in the range 300-1800 m/z. Automated MS/MS sequencing was carried out between 100-2000 m/z in Q2 pulsing mode. The instrument was externally calibrated using a Csl and [Glu1]-Fibrinopeptide B (Sigma, St. Louis, MO) prior to each set of runs.

Analysis of MS data. A typical MS run resulted in approximately 1500 to 2000 MS/MS spectra. These were converted to a Mascot Generic File using Analyst QS software via a script available from Matrix Sciences ([www.matrixscience.com](http://www.matrixscience.com)). The data was then used to probe the SwissProt human database (update 071807) using three different search engines: MASCOT (Matrix Sciences), Phenyx (GenBio, Geneva Switzerland), and X! Tandem (The Global Proteome Machine, [www.theGPM.org](http://www.theGPM.org)). Each algorithm was used with statistical score cut-off options disabled, an allowance of up to 2 missed tryptic cleavages, 0.15 Da MS and MS/MS accuracy, with oxidized methionines and carboxymethylated cysteines enabled. Protein identifications were considered reliable if they met all of the following conditions: 1) were found in any two of the three search algorithms, 2) contained at

least 2 unique peptides from the putative protein sequence, 3) the MS/MS evidence was judged to be plausible for the identification (typically about 50% of expected y- or b-series ions present). Criteria 2 was applied across samples and HDL subfractions.

Western blotting for apoF. HDL subfractions (eight micrograms of protein per lane) were subjected to denaturing SDS-PAGE on pre-cast 12% Bis-Tris gels (Invitrogen). Proteins were electrophoretically transferred to nitrocellulose membranes.

Membranes were blocked for one hour in blocking solution (5% nonfat dry milk in PBS with 0.05% Tween 20). Rabbit anti-human Apo F antisera raised against virally expressed full length human Apo F was added in a 1: 5,000 dilution in blocking solution and incubated overnight at 4°C. Membranes were washed and donkey anti-rabbit IgG conjugated to horseradish peroxidase secondary antibody (Amersham) was added in a 1:5000 dilution in blocking solution and incubated for 3 hours.

Membranes were washed again as before, and proteins were visualized on autoradiography film by chemiluminescence using ECL reagent (Amersham).

Validation of the MS analysis and protein identification strategy. The identification strategy listed in *Methods* was verified using the Universal Proteomics Standard (Sigma) which contains a mixture of 48 purified human proteins. Using the same protocol, including the delipidation procedure, a blinded operator correctly identified 43 of the proteins. Importantly, the stringent identification criteria resulted in 0 false positive identifications. An additional 3 proteins would have been correctly identified, but the presence of only one unique peptide precluded them from the final identification list. Thus, our analysis strategy may exclude some proteins, especially those of extremely low abundance, but is unlikely to indicate the presence of proteins that are not truly present in the samples.

Statistical analysis. All data are shown as means  $\pm$  1 sample standard deviation.

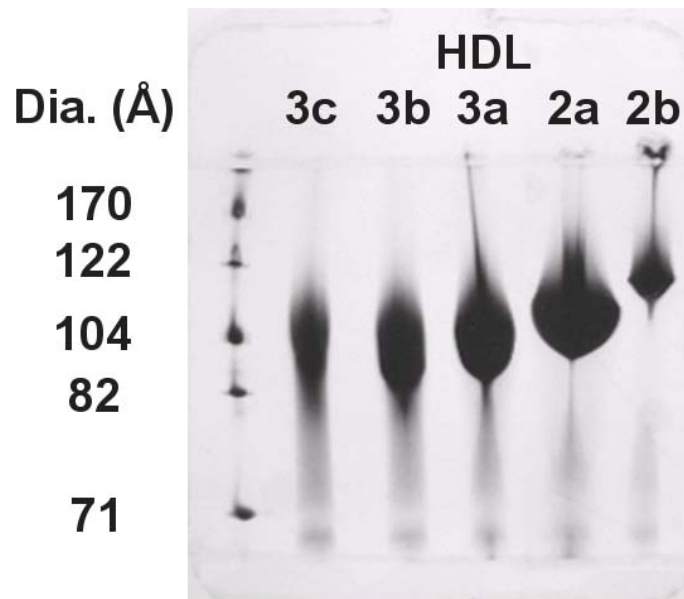
Pearson's moment-product correlation coefficients were calculated to evaluate relationships between variables. Correlations among HDL proteins across the density subfractions were additionally analyzed using the organic algorithm of the Cytoscape software package. The nodes (HDL-associated proteins) were laid out and modified to cluster highly correlated nodes in close proximity. The nodes were treated like physical objects with mutually repulsive forces connected by metal springs representing the experimentally derived correlations between the nodes. The algorithm arranges the nodes so that the sum of the forces emitted by the nodes and the edges reaches a local minimum.

## References

1. Kontush A, Chantepie S, Chapman MJ. Small, dense HDL particles exert potent protection of atherogenic LDL against oxidative stress. *Arterioscler Thromb Vasc Biol.* 2003;23:1881-1888.
2. Mackness MI. Why plasma should not be used to study paraoxonase. *Atherosclerosis.* 1998;136:195-196.
3. Chapman MJ, Goldstein S, Lagrange D, Laplaud PM. A density gradient ultracentrifugal procedure for the isolation of the major lipoprotein classes from human serum. *J Lipid Res.* 1981;22:339-358.
4. Guerin M, Egger P, Le Goff W, Soudant C, Dupuis R, Chapman MJ. Atorvastatin reduces postprandial accumulation and cholesteryl ester transfer protein-mediated remodeling of triglyceride-rich lipoprotein subspecies in type IIb hyperlipidemia. *J Clin Endocrinol Metab.* 2002;87:4991-5000.
5. Guerin M, Le Goff W, Lassel TS, Van Tol A, Steiner G, Chapman MJ. Atherogenic role of elevated CE transfer from HDL to VLDL(1) and dense LDL in type 2 diabetes: impact of the degree of triglyceridemia. *Arterioscler Thromb Vasc Biol.* 2001;21:282-288.
6. Kontush A, Therond P, Zerrad A, Couturier M, Negre-Salvayre A, de Souza JA, Chantepie S, Chapman MJ. Preferential sphingosine-1-phosphate enrichment and sphingomyelin depletion are key features of small dense HDL3 particles: relevance to antiapoptotic and antioxidative activities. *Arterioscler Thromb Vasc Biol.* 2007;27:1843-1849.
7. Hansel B, Giral P, Nobecourt E, Chantepie S, Bruckert E, Chapman MJ, Kontush A. Metabolic syndrome is associated with elevated oxidative stress

and dysfunctional dense high-density lipoprotein particles displaying impaired antioxidative activity. *J Clin Endocrinol Metab.* 2004;89:4963-4971.

## Figures and Tables



### Online Figure I. Native polyacrylamide gel analysis of HDL density subclasses.

10  $\mu$ g of total HDL protein for each subfraction was loaded onto an Amersham Phast 8-25% native gel and run for 264 aVh. The gel was stained with Coomassie blue. Amersham HMW standards were used in lane 1.

**Online Table I.** Chemical properties and antioxidative activity of HDL subfractions<sup>a</sup>

Subfraction	Density range (g/ml)	Avg. Dia. (nm)	Average chemical composition (%) Protein/PL/FC/CE/TG	Antioxidative capacity of HDL (% decrease in the LDL propagation rate) <sup>b</sup>
HDL2b	1.063 – 1.087	10.4	33/30/4/29/4	-2 ± 7
HDL2a	1.088 – 1.110	10.3	34/33/3/27/4	10 ± 9
HDL3a	1.111 – 1.129	9.9	41/29/2/24/3	17 ± 8
HDL3b	1.130 – 1.154	8.0	50/24/1/23/2	33 ± 7
HDL3c	1.155 – 1.170	7.3	66/16/<1/17/1	70 ± 3

<sup>a</sup> Information reprinted from <sup>1</sup>.

<sup>b</sup> Oxidation of total LDL in the presence of individual HDL subfractions was performed *in vitro* in the presence of the azo-initiator, AAPH. Antioxidative capacity of HDL is presented as a decrease in the oxidation rate in the propagation phase of LDL oxidation, during which the inhibitory action of HDL is particularly potent.<sup>1</sup> Data are shown for four healthy normolipidemic donors.

**Online Table II.** Peptide count data for HDL subfractions derived from individual normolipidemic donors (n=9).

		SUM					Average					Standard Deviation				
		3c	3b	3a	2a	2b	3c	3b	3a	2a	2b	3c	3b	3a	2a	2b
A1AT	alpha1 anti-trypsin	12	0	0	0	0	1.3	0.0	0.0	0.0	0.0	1.9	0.0	0.0	0.0	0.0
APOA	apolipoprotein (a)	1	0	0	17	29	0.1	0.0	0.0	1.9	3.2	0.3	0.0	0.0	5.0	4.2
APOA1	apolipoprotein A-I	442	455	489	444	438	49.1	50.6	54.3	49.3	48.7	13.2	10.0	22.8	16.5	19.4
APOA2	apolipoprotein A-II	89	99	113	107	95	9.9	11.0	12.6	11.9	10.6	4.4	3.2	3.1	3.6	4.5
APOA4	apolipoprotein A-IV	7	0	0	0	2	0.8	0.0	0.0	0.0	0.2	1.3	0.0	0.0	0.0	0.4
APOB	apolipoprotein B	84	11	0	52	686	9.3	1.2	0.0	5.8	76.2	25.1	2.4	0.0	10.3	41.7
APOC1	apolipoprotein C-I	42	45	52	58	51	4.7	5.0	5.8	6.4	5.7	1.4	1.3	1.2	1.2	2.0
APOC2	apolipoprotein C-II	15	17	22	28	34	1.7	1.9	2.4	3.1	3.8	1.4	1.3	1.3	1.8	1.4
APOC3	apolipoprotein C-III	20	21	26	23	26	2.2	2.3	2.9	2.6	2.9	1.2	1.2	1.5	1.7	1.7
APOC4	apolipoprotein C-IV	2	1	1	2	3	0.2	0.1	0.1	0.2	0.3	0.7	0.3	0.3	0.7	1.0
APOD	apolipoprotein D	60	58	44	30	27	6.7	6.4	4.9	3.3	3.0	1.9	1.7	1.3	2.3	2.0
APOE	apolipoprotein E	106	78	63	90	170	11.8	8.7	7.0	10.0	18.9	5.4	5.8	6.7	7.0	8.2
APOF	apolipoprotein F	12	8	2	0	0	1.3	0.9	0.2	0.0	0.0	1.2	0.8	0.4	0.0	0.0
APOL1	apolipoprotein L-I	125	73	8	5	3	13.9	8.1	0.9	0.6	0.3	6.1	6.6	2.3	1.7	1.0
APOM	apolipoprotein M	80	88	65	29	18	8.9	9.8	7.2	3.2	2.0	1.7	1.6	2.6	3.2	3.0
CLUS	apolipoprotein J	13	1	0	0	0	1.4	0.1	0.0	0.0	0.0	1.4	0.3	0.0	0.0	0.0
PLTP	Phospholipid transfer protein	15	13	1	1	0	1.7	1.4	0.1	0.1	0.0	1.4	1.9	0.3	0.3	0.0
PON1	Paraoxonase 1	64	26	3	0	0	7.1	2.9	0.3	0.0	0.0	4.1	3.5	1.0	0.0	0.0
PON3	Paraoxonase 3	12	5	0	0	0	1.3	0.6	0.0	0.0	0.0	1.1	0.9	0.0	0.0	0.0
SAA	Serum amyloid A (1 and 2)	18	27	15	7	7	2.0	3.0	1.7	0.8	0.8	2.4	2.5	1.9	0.7	0.7
SAA4	Serum amyloid A 4	65	75	66	63	57	7.2	8.3	7.3	7.0	6.3	3.2	2.0	2.1	1.9	1.6
LIS1	PAF-AH IB subunit alpha	1	3	3	1	3	0.1	0.3	0.3	0.1	0.3	0.3	0.5	0.5	0.3	0.5
ALBU	Albumin	16	0	0	0	5	1.8	0.0	0.0	0.0	0.6	3.0	0.0	0.0	0.0	1.7
FIBA	Fibrinogen alpha chain	3	0	0	0	0	0.3	0.0	0.0	0.0	0.0	0.7	0.0	0.0	0.0	0.0
HPTR	Haptoglobin related protein	13	0	0	0	0	1.4	0.0	0.0	0.0	0.0	2.3	0.0	0.0	0.0	0.0
PAFA	Platelet-activating factor acetylhydrolase	0	0	0	0	1	0.0	0.0	0.0	0.0	0.1	0.0	0.0	0.0	0.0	0.3
SCYB7	Platelet basic protein	6	6	2	0	0	0.7	0.7	0.2	0.0	0.0	1.7	1.0	0.7	0.0	0.0
THRB	Prothrombin	4	2	0	1	0	0.4	0.2	0.0	0.1	0.0	1.3	0.7	0.0	0.3	0.0
TTHY	Transthyretin	3	0	0	0	0	0.3	0.0	0.0	0.0	0.0	0.7	0.0	0.0	0.0	0.0

**Online Table III.** Peptide count data for HDL subfractions derived from three samples, each containing pooled plasma from 20 normolipidemic donors (n=3).

		SUM					Average					Standard Deviation				
		3c	3b	3a	2a	2b	3c	3b	3a	2a	2b	3c	3b	3a	2a	2b
A1AT	alpha1 anti-trypsin															
APOA	apolipoprotein (a)	1	0	0	0	0	0.3	0.0	0.0	0.0	0.0	0.6	0.0	0.0	0.0	0.0
APOA1	apolipoprotein A-I	0	0	0	0	7	0.0	0.0	0.0	0.0	2.3	0.0	0.0	0.0	0.0	1.2
APOA2	apolipoprotein A-II	224	238	259	229	210	74.7	79.3	86.3	76.3	70.0	45.1	38.9	37.5	39.8	38.4
APOA4	apolipoprotein A-IV	25	24	30	32	22	8.3	8.0	10.0	10.7	7.3	0.6	0.0	1.0	2.3	1.5
APOB	apolipoprotein B	1	0	0	0	0	0.3	0.0	0.0	0.0	0.0	0.6	0.0	0.0	0.0	0.0
APOC1	apolipoprotein C-I	1	0	0	0	254	0.3	0.0	0.0	0.0	84.7	0.6	0.0	0.0	0.0	35.8
APOC2	apolipoprotein C-II	10	10	13	16	17	3.3	3.3	4.3	5.3	5.7	0.6	1.5	1.5	3.1	2.5
APOC3	apolipoprotein C-III	2	3	11	13	13	0.7	1.0	3.7	4.3	4.3	0.6	0.0	1.5	0.6	1.5
APOC4	apolipoprotein C-IV	8	10	13	14	15	2.7	3.3	4.3	4.7	5.0	0.6	0.6	0.6	0.6	1.0
APOD	apolipoprotein D	3	2	1	2	3	1.0	0.7	0.3	0.7	1.0	0.0	0.6	0.6	0.6	1.0
APOE	apolipoprotein E	17	21	13	10	3	5.7	7.0	4.3	3.3	1.0	1.5	1.0	0.6	0.6	1.0
APOF	apolipoprotein F	33	31	22	24	47	11.0	10.3	7.3	8.0	15.7	7.0	3.8	1.2	1.7	5.7
APOL1	apolipoprotein L-I	9	5	2	0	0	3.0	1.7	0.7	0.0	0.0	1.7	0.6	0.6	0.0	0.0
APOM	apolipoprotein M	26	20	0	0	0	8.7	6.7	0.0	0.0	0.0	4.0	1.2	0.0	0.0	0.0
CLUS	apolipoprotein J	25	28	19	6	3	8.3	9.3	6.3	2.0	1.0	2.1	1.2	5.5	2.0	1.0
PLTP	Phospholipid transfer protein	2	6	2	0	0	0.7	2.0	0.7	0.0	0.0	0.6	2.6	1.2	0.0	0.0
PON1	Paraoxonase 1	5	5	1	0	0	1.7	1.7	0.3	0.0	0.0	1.5	2.1	0.6	0.0	0.0
PON3	Paraoxonase 3	10	5	0	0	0	3.3	1.7	0.0	0.0	0.0	3.1	1.5	0.0	0.0	0.0
SAA	Serum amyloid A (1 and 2)	4	0	0	0	0	1.3	0.0	0.0	0.0	0.0	1.5	0.0	0.0	0.0	0.0
SAA4	Serum amyloid A 4	5	7	4	3	3	1.7	2.3	1.3	1.0	1.0	1.5	1.5	1.2	0.0	0.0
LIS1	PAF-AH IB subunit alpha	14	16	17	15	19	4.7	5.3	5.7	5.0	6.3	1.2	1.5	2.5	1.0	1.2
ALBU	Albumin	2	4	2	1	1	0.7	1.3	0.7	0.3	0.3	1.2	1.5	0.6	0.6	0.6
FIBA	Fibrinogen alpha chain	0	0	0	0	0	0.0	0.0	0.0	0.0	0.0	0.0	0.0	0.0	0.0	0.0
HPTR	Haptoglobin related protein	0	0	0	0	0	0.0	0.0	0.0	0.0	0.0	0.0	0.0	0.0	0.0	0.0
PAFA	Platelet-activating factor acetylhydrolase	0	0	0	0	0	0.0	0.0	0.0	0.0	0.0	0.0	0.0	0.0	0.0	0.0
SCYB7	Platelet basic protein	0	0	0	0	0	0.0	0.0	0.0	0.0	0.0	0.0	0.0	0.0	0.0	0.0
THRB	Prothrombin	0	0	0	0	0	0.0	0.0	0.0	0.0	0.0	0.0	0.0	0.0	0.0	0.0

